PHILOSOPHICAL TRANSACTIONS OF THE ROYAL SOCIETY A MATHEMATICAL, PHYSICAL & ENGINEERING SCIENCES

Ultrafast spectroscopy of the electron transfer in photosynthetic reaction centres: towards a better understanding of electron transfer in biological systems

W. Zinth, P. Huppmann, T. Arlt and J. Wachtveitl

Phil. Trans. R. Soc. Lond. A 1998 **356**, 465-476
doi: 10.1098/rsta.1998.0176

The Royal Society

Ultrafast spectroscopy of the electron transfer in photosynthetic reaction centres: towards a better understanding of electron transfer in biological systems

By W. Zinth, P. Huppmann, T. Arlt and J. Wachtveitl

Institut für Medizinische Optik, Ludwig-Maximilians-Universität München, Dettingenstrasse 67, 80538 München, Germany

Femtosecond spectroscopy shows that primary electron transfer in photosynthetic reaction centres is an ultrafast stepwise reaction where the electron is transferred via a chain of pigments. In a first reaction step, the electron is transferred from the special pair to the accessory bacteriochlorophyll with a time constant of *ca.* 3 ps. A second, subpicosecond reaction carries the electron to a bacteriopheophytin before it reaches the quinone Q_A within 200 ps. Experiments on native and mutated reaction centres yield information on energetics, reorganization energies and electronic coupling. A consistent theoretical treatment of the data shows that standard non-adiabatic theory describes well the primary electron transfer process at room temperature. However, for a special fast reacting mutant at low temperatures, the limits of non-adiabatic theory may be reached.

Keywords: adiabatic electron transfer; non-adiabatic electron transfer; optimization of photosynthesis; primary photosynthesis; reaction mechanisms

1. Introduction

The photosynthetic conversion of sunlight into chemical energy is either directly or indirectly the major energy source for all organisms. It is not surprising therefore that photosynthesis has been a topic of general scientific interest since the early days of modern natural science. The major principles of the biochemical 'dark reactions' with the final energy storage in long-lived energy-rich compounds have been well understood in the past (for a review, see Clayton 1978). More recent developments in photosynthetic research focus on the primary photophysical events where light energy is collected by antenna systems, transferred to the reaction centres (RC) and initially stored via a transmembrane electron transfer (ET) process. The present progress in the understanding of these 'light reactions' is connected with the synergetic action from the three different fields of research: structure analysis, ultrafast spectroscopy and protein engineering.

(*a*) *Structural analysis*

Since the first resolution of the molecular structure of a reaction centre from *Rps. viridis* at the atomic level by Deisenhofer, Huber and Michel in 1985 (Deisenhofer *et al.* 1985; Deisenhofer & Michel 1989), the basic elements of the primary electron

transfer reaction have been known. Structural analysis of other photosynthetic organisms (Chang *et al.* 1986; Ermler *et al.* 1994) has revealed that the same key elements are used for primary electron transfer: the primary electron donor is a pair of (bacterio)chlorophyll molecules called the special pair, P. The structure suggests that the subsequent electron flow occurs via the neighbouring accessory bacteriochlorophyll (BChl), the bacteriopheophytin (BPhe) H, to the quinone Q. Surprisingly, two potential electron transfer chains (indices A and B) are found:

$$\mathrm{P} \rightarrow \mathrm{B_A} \rightarrow \mathrm{H_A} \rightarrow \mathrm{Q_A}, \tag{1.1}$$

$$\mathrm{P} \rightarrow \mathrm{B_B} \rightarrow \mathrm{H_B} \rightarrow \mathrm{Q_B}. \tag{1.2}$$

These two branches are arranged in an approximate C_2 symmetry (see upper part of figure 1). Experimental data on RC of purple bacteria have shown that one pigment chain—the A branch—is predominantly used for electron transfer. This was first deduced from polarized spectroscopy of crystallized reaction centres where, in the absence of the quinone $\mathrm{Q_B}$, the radical pair state $\mathrm{P^+Q_A^-}$ was formed with high efficiency (Zinth *et al.* 1983, 1985; Knapp *et al.* 1985). Later, the functional asymmetry was confirmed by direct time-resolved spectroscopy at low temperatures in the absorption bands of $\mathrm{H_A}$ and $\mathrm{H_B}$ (Kirmaier *et al.* 1985; Michel-Beyerle *et al.* 1988).

The recent determination of the structure of light harvesting antenna systems (McDermott *et al.* 1995) exhibited an extremely symmetric arrangement where ultrafast subpicosecond energy transfer occurs within the light harvesting complex. In addition, the arrangement allows fast energy transfer between different light harvesting complexes as well as from these complexes to the reaction centre.

(*b*) *Ultrafast spectroscopy*

The development of spectroscopic methods throughout the whole visible and near infrared with a time resolution on the timescale of the photosynthetic electron transfer processes allows one to follow directly the dynamics of the electron transfer reactions and the sequence of intermediate states. The most detailed information has been obtained for bacterial reaction centres where the light harvesting pigments are removed completely. Here the reaction dynamics can be followed without interference from energy transfer processes. Experiments performed in 1986 have shown that the decay of the excited electronic state $\mathrm{P^*}$ and the associated first electron transfer away from P occur within 3 ps (Martin *et al.* 1986; Breton *et al.* 1986). With the same time constant, the electron arrives at the BPhe H_A. Since no indication for an intermediate state $\mathrm{P^+B_A^-}$ with the electron at the accessory BChl $\mathrm{B_A}$ was found, the electron transfer was assumed to follow a superexchange mechanism with direct transfer to $\mathrm{H_A}$ (Martin *et al.* 1986; Breton *et al.* 1986; Kirmaier & Holten 1990). Subsequently, the observation of a distinct subpicosecond kinetic component with pronounced amplitudes in the spectral ranges with high absorption of BChl and $\mathrm{BChl^-}$ strongly suggested a stepwise electron transfer via $\mathrm{B_A}$ with a real population of the intermediate $\mathrm{P^+B_A^-}$ (Holzapfel *et al.* 1989, 1990; Arlt *et al.* 1993; Dressler *et al.* 1991; Chan *et al.* 1991; Beekman *et al.* 1995),

$$\mathrm{P^*} \overset{\tau_1=3\ \mathrm{ps}}{\longrightarrow} \mathrm{P^+B_A^-} \overset{\tau_2=0.9\ \mathrm{ps}}{\longrightarrow} \mathrm{P^+H_A^-} \overset{\tau_3=200\ \mathrm{ps}}{\longrightarrow} \mathrm{P^+Q_A^-}. \tag{1.3}$$

Even if a large body of experimental evidence supports the stepwise electron transfer model, it has been not generally accepted to date.

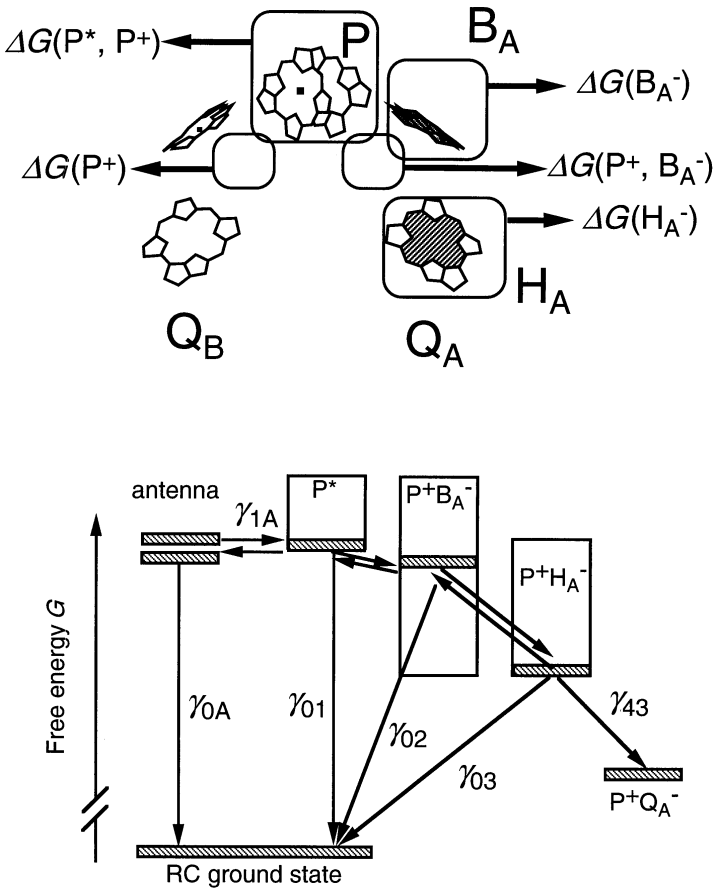

Figure 1. (Top) Scheme of the chromophores of bacterial reaction centres. Electron transfer starts at the primary donor P and uses the active A branch of chromophores. The boxes indicate the locations where modifications have been introduced in the past in order to change the free energy ΔG of intermediate states. (Bottom) Reaction scheme for the primary photosynthetic processes with the reaction rates γ_{ij} coupling the different states. The efficiency of the electron transfer strongly depends on the interplay between forward and recombination rates.

(*c*) *Protein engineering*

Protein engineering with site directed mutagenesis or pigment exchange permits well-defined modifications of the functional parts of the reaction centre. The distinct variation of the parameters controlling electron transfer leads to an improved understanding of the electron transfer mechanisms and allows an experimental check of electron transfer theories.

In this paper we want to address the reaction mechanisms and pathways of the primary electron transfer in bacterial reaction centres. We present data showing that $P^+B_A^-$ is involved in primary electron transfer as a real intermediate. Results on a variety of mutated reaction centres also support the idea of stepwise electron transfer via $P^+B_A^-$. We will show that the room temperature reactions can be described well by non-adiabatic electron transfer theory while electron transfer at low temperatures in a fast reacting mutant is at, or beyond, the limits of non-adiabatic electron transfer theory.

2. Material and methods

The time-resolved experiments are performed using the pump and probe technique. The experiments use a subpicosecond laser-amplifier system described elsewhere (Arlt *et al.* 1993). Subpicosecond, weak (less than 15% excitation of the sample) and short ($t_P \approx 150$ fs) light pulses at wavelengths in the Q_y band of the special pair are used to initiate electron transfer. Properly delayed probing pulses at a variety of visible and near infrared probing wavelengths λ_{pr} are obtained by continuum generation. They measure the absorbance changes as a function of delay time t_D. The sample concentration is adjusted to yield a transmission $T \approx 10\%$ in the special pair Q_y band. The time-resolved absorption data are analysed using a rate-equation model for the electron transfer reaction. The details of the data evaluation procedure have been described elsewhere (Schmidt *et al.* 1995; Finkele *et al.* 1990).

Preparation and isolation of the RC is described in Arlt *et al.* (1996*a*,*b*). For the low-temperature experiments, glycerol (54% v/v) was used as a cryoprotector. Benzyl viologen (0.15 g per ml sample) served to prevent accumulation of long-lived intermediates. The modifications of the RC used in these experiments are designed to vary the difference in free energy between the excited electronic state P^*, the first intermediate $P^+B_A^-$ and the second intermediate $P^+H_A^-$. These variations concern different locations in the RC, as shown schematically by the boxes in the upper part of figure 1. (i) Mutations in the binding pocket of the special pair (e.g. L168H → F) may change the energetics ΔG of P^* as well as that of all P^+ containing intermediates. (ii) Mutations in the surrounding of B_A influence the energetics of the state $P^+B_A^-$. (iii) Chromophore exchange at B and H tune the energy differences between $P^+B_A^-$ and $P^+H_A^-$. The range of free energies covered by the modifications is indicated by the rectangles in figure 1, lower part.

3. Time-resolved spectroscopy on bacterial reaction centres: electron transfer is a stepwise reaction

Femto- and picosecond experiments have been performed on a variety of bacterial RC. Here we will summarize the observations found for RC of *Rb. sphaeroides* and *Rps. viridis*. RC from *Rb. capsulatus* and *Rsp. rubrum* gave similar results. We discuss the data in the context of a rate-equation model with a certain number N of intermediate states I_i coupled via transition rates γ. The rate γ_{ij} represents the transfer from intermediate I_j to I_i. This model yields the appropriate mathematical description for standard non-adiabatic ET theory. Here, populations and absorption changes are described by exponentials where the decay times τ_n are related to the rates γ_{ij}. The number of time constants directly reflects the number of intermediates involved (Schmidt *et al.* 1995; Arlt *et al.* 1996*a*). For a sequential and unidirectional model like the one shown in equation (1.3), the decay time of a state I_m is given directly by $\tau_m = 1/\gamma_{nm}$. The experimental data, measured over a wide spectral range in the visible and infrared, yield at 300 K the time constants *ca.* 3, *ca.* 0.9 (in *Rps. viridis*, 0.65 ps), 200 ps and infinity. The amplitudes related with these decay times have very different spectral signatures. In addition to the four time constants given above, another time constant, 7 ps, could be resolved in the experiments. Upon introduction of the additional 7 ps component, the 3 ps time constant is reduced to 2.3 ps (*Rb. sphaeroides*) and 1.8 ps (*Rps. viridis*). Its amplitudes are weak and the associated spectral properties follow those of the 3 ps kinetic component. These

observations suggest that the two time constants (2.3 and 7 ps) describe two fractions of RC, where potential variations in the protein surrounding tune the reaction rate. In the following we will discuss only the 3 ps component. Considering the additional 7 and 2.3 ps components leads to the same conclusions.

The 3 ps kinetic component shows all signatures of a decay of the excited electronic state P^*: with the 3 ps process one finds the decrease of spontaneous emission, the decay of stimulated emission or gain and the disappearance of excited state absorption. With the same time constant, a charge separated state containing P^+ is formed. On the same time scale the features related with intermediate $P^+H_A^-$ (bleach of H_A bands, electrochromic shifts of BChl bands) appear. The 3 ps component is therefore assigned to the decay of P^* and the initial ET away from P.

The 200 ps kinetic component exhibits properties related to the reappearance of the H_A absorption. It can be assigned to the final picosecond ET to the quinone Q_A where the electron remains for a long time (infinity on our time scale).

Of special interest is the 0.9 ps kinetic component which has pronounced amplitudes only at distinct spectral positions known to represent BChl or its anion.

The spectrally resolved absorption data can be used to calculate the difference absorption spectra of the intermediate states provided the reaction model is known. Assuming a sequential reaction model without back reaction (an assumption which is justified considering the energetics given below) in combination with the sequence of processes in the order of 3, 0.9, 200 ps and ∞, the difference spectra shown in figure 2 are obtained. The spectra of the initial intermediate (figure 2*b*), the third intermediate (figure 2*d*) and the final picosecond intermediate (figure 2*e*) closely resemble the spectra expected for P^*, $P^+H_A^-$ and $P^+Q_A^-$, respectively. Of special interest is the spectrum of the second intermediate (figure 2*c*); it contains features related to the cation P^+ (bleach of the P band) together with features characteristic for the BChl anion state: increased absorption at 660 and 1020 nm, bleach at 800 nm. All signatures observed in an *in vitro* difference spectrum of the BChl-a anion (broken curve, redrawn from Fajer *et al.* (1975) after a 20 nm shift to longer wavelengths used to account for solvent shifts) are reproduced in the difference spectrum of intermediate I_2 which we assign to the state $P^+B_A^-$. The spectral dependencies therefore strongly support a stepwise ET model in the bacterial RC according to equation (1.3) where the electron resides for a short but finite time of 0.9 ps on the accessory BChl B_A.

4. Energetics of the first intermediate state $P^+B_A^-$

A sequential ET via the BChl B_A imposes restrictions on the energetics of the related intermediate $P^+B_A^-$. Only if the energy of $P^+B_A^-$ is close to P^* or somewhat below P^* can efficient and fast ET become possible. A state $P^+B_A^-$ well above P^* cannot play a role in a stepwise ET scheme. It can only support ET in a superexchange model where state $P^+H_A^-$ is reached within one reaction step. The most direct way to determine the energetics of $P^+B_A^-$ was realized in a modified RC of *Rb. sphaeroides* where the secondary electron acceptor H_A, a BPhe molecule, was replaced by a pheophytin (Schmidt *et al.* 1994). The exchange should leave the position of B_A and energetics of $P^+B_A^-$ unchanged, but allows via the energetically lifted high-lying state $P^+H_A^-$ to measure long-lived (*ca.* 300 ps) populations of P^*, $P^+B_A^-$ and $P^+H_A^-$ in thermal equilibrium. From the analysis of these data, the energetics of $P^+B_A^-$ could be determined. A value of $\Delta G(P^+B_A^-) = -450\,\mathrm{cm}^{-1}$ (with respect to $\Delta G(P^*)$) was found, which means that the state $P^+B_A^-$ is $450\,\mathrm{cm}^{-1}$ below P^*, as

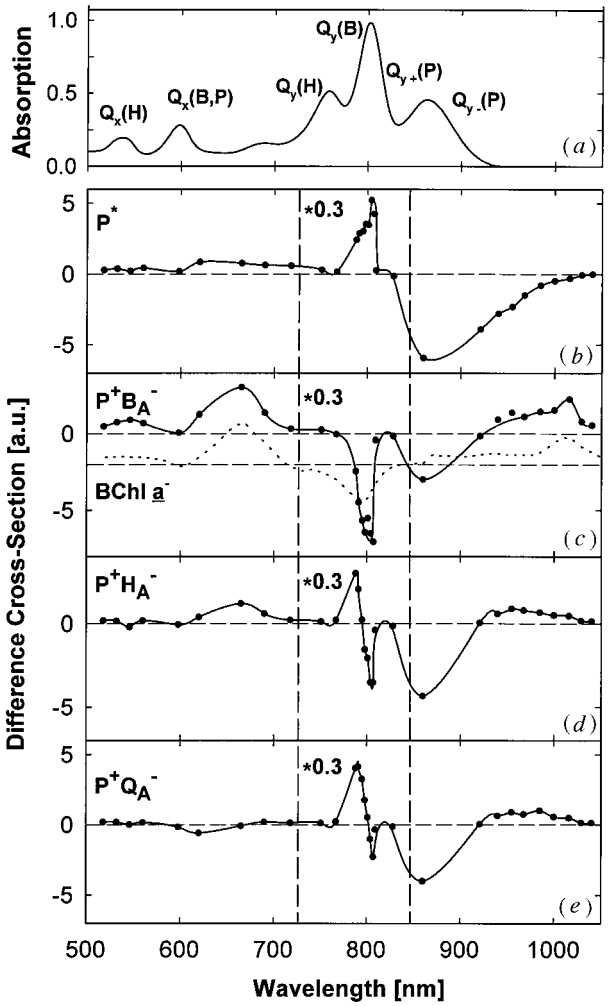

Figure 2. Spectra of the reaction centres of *Rb. sphaeroides*: (*a*) stationary absorption spectrum; (*b*)–(*e*) spectra of the intermediates in the primary photosynthetic electron transfer (solid lines and points); in figure 1*c*, the absorption difference spectrum for the bacteriochlorophyll anion (Fajer *et al.* 1975) is shown as the dotted curve.

expected for a stepwise ET model. This value was confirmed in a detailed analysis of the results from a series of RC mutants of *Rb. sphaeroides*, where the energy gap between P^* and $P^+B_A^-$ was changed (Bixon *et al.* 1995, 1996). This analysis yielded the energy of the first intermediate states in wild-type RC to be $\Delta G \approx -480\ \mathrm{cm}^{-1}$, in good agreement with the above-mentioned value. In addition, the analysis indicated that primary ET is connected with a relatively weak reorganization energy of $\lambda \approx 800\ \mathrm{cm}^{-1}$.

Figure 3 gives the results for a related analysis for the RC of *Rps. viridis*. Here the fast time constant of the primary reaction of a series of mutants is plotted versus the free energy $\Delta G(P^+B_A^-)$ of the first intermediate. The energetic positions of the mutants relative to the wild type were determined independently via redox measurements or from the temperature dependence of the reaction rates. The energetics of wild-type RC and the reorganization energy λ (the same value was used for all

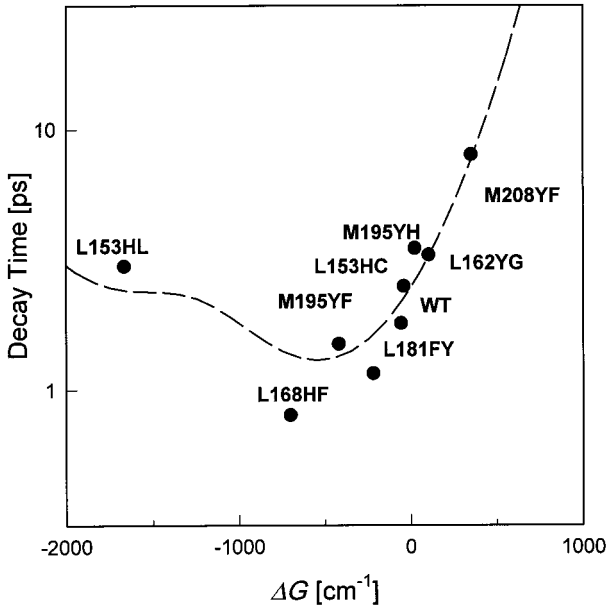

Figure 3. Reaction rates for the primary ET process for a set of mutants of *Rps. viridis* (points) and reaction rates (broken curve) calculated using equation (4.1). The parameters of the ET-process (free energy of state $P^+B_A^-$ for the wild-type RC, reorganization energy λ and electronic coupling) are determined by a least-square fitting procedure.

mutants) were determined by fitting the experimental data to standard non-adiabatic ET theory in a multimode picture (Jortner 1976). A high-frequency intramolecular vibrational mode at $\hbar\omega' = 1200\,\mathrm{cm}^{-1}$ with a coupling parameter $S \approx 0.5$ was considered in addition to the low-frequency intermolecular mode $\hbar\omega$,

$$\frac{1}{\tau_1} = \gamma_{21} = \frac{2\pi}{\hbar}\frac{V^2}{\sqrt{4\pi\lambda k_\mathrm{B}T}}\mathrm{e}^{-S}\sum_{n=0}^{\infty}\exp\left[-\frac{(\Delta G + \lambda + n\hbar\omega')^2}{4\lambda k_\mathrm{B}T}\right]. \tag{4.1}$$

The calculation yielded an energy of $\Delta G(P^+B_A^-) = -55 \pm 100\,\mathrm{cm}^{-1}$, i.e. $P^+B_A^-$ is nearly isoenergetic to P^*. The reorganization energy $\lambda \approx 500\,\mathrm{cm}^{-1}$ is even smaller than that found in the RC of *Rb. sphaeroides*. The electronic coupling was deduced to be $V \approx 34\,\mathrm{cm}^{-1}$. The variation of $\Delta G(P^+B_A^-)$ in the different mutants cannot only be used to estimate the energetic positions of $P^+B_A^-$ but it also gives independent support for the stepwise ET model. The change in $\Delta G(P^+B_A^-)$ strongly influences the initial ET rate. In addition, it changes the peak population of the intermediate $P^+B_A^-$ (and with that the visibility of the fast 0.9/0.65 ps kinetic component). Furthermore, the quantum yield for the formation of the product state $P^+Q_A^-$ will be influenced. In the experiments on the different mutants one finds that all these parameters are changed in the manner predicted by the stepwise ET model.

5. Mechanisms of primary electron transfer

The analysis of the primary ET given above could explain the experimental observations within the frame of non-adiabatic ET theory. It yielded a consistent description of the experimental results obtained for all investigated mutants at room temperature. In general, the range of non-adiabatic theory can be controlled via the

Landau–Zener parameter γ_{LZ} (Bixon *et al.* 1990),

$$\gamma_{LZ} = \frac{2\pi V^2}{\hbar\omega\sqrt{2\lambda k_B T}}, \tag{5.1}$$

where $\hbar\omega \approx 100\,\mathrm{cm}^{-1}$ (Lauterwasser *et al.* 1991) is the frequency of the relevant low-frequency mode and V is the electronic coupling ($V \approx 30\,\mathrm{cm}^{-1}$). A value of $\gamma_{LZ} \ll 1$ represents non-adiabatic ET theory. For room temperature $k_B T \approx 210\,\mathrm{cm}^{-1}$ we estimate a value of $\gamma_{LZ} \approx 0.1$. Even for the faster secondary ET step with $V \approx 60\,\mathrm{cm}^{-1}$, $\lambda = 1200\,\mathrm{cm}^{-1}$, we find values of $\gamma_{LZ} \approx 0.3$ still within the non-adiabatic regime. Thus, under the physiological conditions of room temperature, the electron transfer reaction is well described by the standard non-adiabatic ET theory. For low temperatures and extremely fast reacting mutants, however, the limits of standard theory may be reached. Interestingly, the RC mutant L168H → F of *Rps. viridis*, which reacts at room temperature much faster than wild type (Arlt *et al.* 1996*b*), is the ideal candidate to explore these limits. The time-resolved absorption changes on the mutated RC L168H → F measured at 1020 nm, in the spectral range of stimulated emission of *Rps. viridis* are shown in figure 4 for 295 and 30 K. At room temperature, the decay of the signal is described (in a biexponential fit) by a 0.8 ps (80%) and a 2.3 ps (20%) kinetic component. The fast process is strongly accelerated at low temperatures. The related temperature dependence of the fast kinetic component is shown in the insert in figure 4: the main reduction of reaction time occurs between 300 and 160 K. At lower temperatures, the reaction time stays practically constant at 250 fs. These experimental observations cannot be explained by standard ET models with constant reaction parameters. Variations in ΔG do not appear to increase sufficiently the reaction rate. However, the observed acceleration can be related to an increase of the electronic coupling or a decrease in the reorganization energy λ. Both changes influence (for a non-activated ET reaction) the reaction rate and the Landau–Zener parameter in the same way. Since the reaction rate depends stronger on V than on λ, we suppose that an increase in V could account for the observation. This increase may happen in two steps.

(1) In the mutant at room temperature the electronic coupling is stronger than in wild-type RC: even at room temperature, the fast rate of this mutant is not fully explained by the fit with a fixed value $V = 34\,\mathrm{cm}^{-1}$ used in figure 2. Since the action of the mutation, the removal of a hydrogen bond to the special pair, could influence the position of P relative to B, an increase of V by a factor of *ca.* 1.5 cannot be excluded.

(2) The electronic coupling increases upon cooling: further increase of V upon cooling by a factor of 2 could explain the rise in reaction rates until 160 K. Using the standard distance dependence of V, $V(r) = V_0 \exp(-0.7\mathrm{A}^{-1} r)$, the increase of V by a factor of 2 would be related to a large change in distance of *ca.* 1A. Considering the anomalies found in the temperature dependent ET rates in wild-type RC and strong changes in structural dynamics measured via Mößbauer experiments in this temperature range (Fleming *et al.* 1988; Frolov *et al.* 1996), the changes in distance suggested above are not unreasonable.

The total increase in electronic coupling would lead to a value of $V \approx 70\,\mathrm{cm}^{-1}$ at 150 K. Calculating the Landau–Zener parameter for this temperature we obtain $\gamma_{LZ} \approx 1$. This value represents a reaction in the range of adiabatic ET theory. The large value of parameter γ_{LZ} suggests that only few (*ca.* 1) crossings of the interaction region are required for the electron transfer reaction to take place. Under

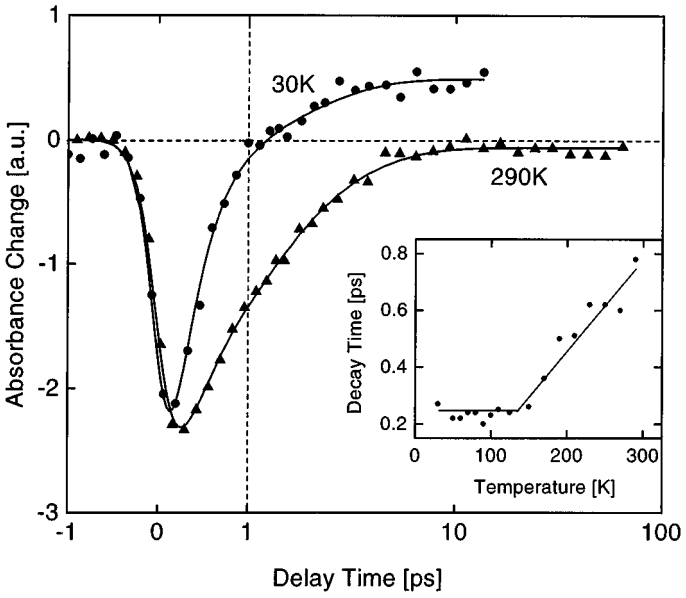

Figure 4. Time-resolved absorption data (points) for RC from the mutant L168H → F of *Rps. viridis* for a probing wavelength of 1020 nm (temperatures 295 and 30 K). The curves are calculated model functions. A linear scale of the delay time is used for $t_D < 1$ ps; a logarithmic scale is applied at later delay times. The insert gives the temperature dependence of the fast kinetic component.

these conditions, the reaction is mainly determined by the frequency of the nuclear vibration and the limits of non-adiabatic ET theory are reached. In this case, even a further increase in electronic coupling would not influence the ET time τ_{ET} which is largely determined by the vibrational period, $\tau_{ET} \approx 1/\nu$. For $\nu/c \approx 100\,\mathrm{cm}^{-1}$, one deduces $\tau_{ET} \approx 330$ fs close to the experimentally found time constant of 250 fs. The absence of a further increase of the reaction rate at even lower temperatures again supports this interpretation.

6. Optimization of primary photosynthesis

Over the past three billion years, photosynthesis has been continuously improved by evolution. Under these conditions, it is not surprising that the present photosynthetic systems are highly optimized. The principles of optimization and the way how these principles are realized will now be discussed. We will concentrate on photosynthetic RC at room temperature and will define efficiency in terms of the fraction η_Q of RC reaching the intermediate $P^+Q_A^-$. However, we will also consider energy transfer from the antenna to the RC which may strongly influence the overall photosynthetic efficiency. For the discussion we refer to the simplified reaction scheme of figure 1. We consider explicitly the ET (rate γ_{21}) from P^* to $P^+B_A^-$ according to equation (4.1). In order to simplify the estimate we use a constant forward reaction rate γ_{32} for the secondary ET from $P^+B_A^-$ to $P^+H_A^-$ justified by the experimental result that this rate does not change significantly for the investigated mutants. Backreactions are described by the principle of detailed balance:

$$\gamma_{ij} = \gamma_{ji} \exp\left(-\frac{\Delta G_i - \Delta G_j}{k_B T}\right). \tag{6.1}$$

Recombination channels are considered from the radical pair states $P^+B_A^-$ (γ_{02}) and $P^+H_A^-$ (γ_{03}) to P together with internal conversion from P^* (γ_{01}) or from the antenna (γ_{0A}). The experiments on the different native and modified RC of *Rps. viridis* suggest the following order of magnitude for the different loss rates: $\gamma_{01} \approx 1/100$ ps, $\gamma_{02} \approx 1/100$ ps, $\gamma_{0A} = 1/1$ ns and $\gamma_{03} = 1/10$ ns. Within this model one can calculate the efficiency η_Q as a function of the energies of the intermediates (Kuhn 1986; Zinth *et al.* 1996). A qualitative estimate of the different loss mechanisms can be obtained by the following argument. In the linear reaction model of photosynthesis, the reaction yield for each step in the reaction chain depends on the ratio of forward reaction rate to recombination rate. For the different reaction steps, optimization is realized by adjusting the forward reaction rates and the energetic positions of the intermediates.

(1) The energetic levels of P^* and the antenna have to be adjusted to allow fast energy transfer to the RC and to avoid internal conversion (γ_{0A}) in the antenna.

(2) For the first ET step in the RC, the recombination is dominated by internal conversion of P^* to groundstate P which proceeds with $1/\gamma_{01} \approx 100$ ps. High quantum efficiency requires that the first reaction step is much faster. The value of $1/\gamma_{21} \approx 3$ ps found in the reaction centres points to a small loss of a few percent.

(3) The high speed of the second electron transfer to H_A with a time constant below 1 ps is necessary in view of the recombination from $P^+B_A^-$ (γ_{02}) which is caused by the small separation of bacteriochlorophyll B_A and the special pair P. A larger distance between these pigments (which would be required for a weaker recombination of $P^+B_A^-$) is not possible since it would directly reduce the primary forward reaction speed γ_{21} and with that the efficiency of the first step (see 2).

(4) The high speed of the electron transfer to the low-lying $P^+H_A^-$ also helps to reduce back transfer to the antenna and finally leads to the trapping of excitation in the RC.

(5) The high energy dissipation in the long-lived (i.e. slowly reacting) later intermediates $P^+H_A^-$ and $P^+Q_A^-$ is also related to optimization. For these intermediates, the direct loss channels are slow. Under these conditions recombination can proceed only via thermal excitation of preceding intermediates such as P^*, $P^+B_A^-$. Thermal activation of these earlier intermediate states and the loss via recombination can only be minimized by a large activation energy for backreaction, i.e. by lowering the energy of the later intermediates. Considering a typical (chemical) reaction time of 10^{-4} s from the final intermediate in the ET process, one estimates that the overall energy loss must be larger than 3000 cm^{-1} in order to keep quantum loss in the few percent range. In fact, the value of 3000 cm^{-1} must be increased in order to compensate the action of the fluctuations in the energetics of the primary intermediate $P^+B_A^-$.

(6) Closely neighbouring pigments and well-adjusted energetics in the first intermediates with small reorganization energies lead to fast forward reaction rates. Large spatial separation of the charge in the radical pair states and energy dissipation in later intermediates prevent direct recombination and thermally activated decay channels. This combination of contradictory properties can only be fulfilled if the reaction proceeds via a number of independent reaction steps.

In conclusion, the investigations on native and mutated RC of purple bacteria have shown that primary electron transfer at room temperature is a stepwise process where the electron is transferred via closely spaced chromophores. The fastest electron transfer reaction occurs at room temperature on the 10^{-12} s range and can

still be described by standard non-adiabatic electron transfer theory. Only for special fast reacting mutants and low temperatures the limits of non-adiabatic theory are reached. Since non-adiabatic electron transfer theory is able to describe photosynthesis under physiological conditions (which is the fastest biological electron transfer reaction known to date) there are no indications that non-standard theory should become necessary for the slower electron transfer processes in other biological systems.

The authors thank D. Oesterhelt, M. Bibikova and B. Dohse for supplying us with RC samples of highest quality.

References

Arlt, T., Dohse, B., Schmidt, S., Wachtveitl, J., Laußermair, E., Zinth, W. & Oesterhelt, D. 1996*a* *Biochem.* **35**, 9235.

Arlt, T., Bibikova, M., Penzkofer, H., Oesterhelt, D. & Zinth, W. 1996*b* *J. Phys. Chem.* **100**, 12 060.

Arlt, T., Schmidt, S., Kaiser, W., Lauterwasser, C., Meyer, M., Scheer, H. & Zinth, W. 1993 *Proc. Natn. Acad. Sci. USA* **90**, 11 757.

Beekman, L. M. P., Jones, M. R., van Stokkum, I. H. M. & van Grondelle, R. 1995 In *Photosynthesis: from light to biosphere* (ed. P. Mathis), p. 495. Dordrecht: Kluwer.

Bixon, M., Jortner, J. & Michel-Beyerle, M. E. 1990 In *Perspectives in photosynthesis* (ed. J. Jortner & B. Pullman), p. 325. Dordrecht: Kluwer.

Bixon, M., Jortner, J. & Michel-Beyerle, M. E. 1995 *Chem. Phys.* **197**, 389.

Bixon, M., Jortner, J. & Michel-Beyerle, M. E. 1996 In *Reaction centers of photosynthetic bacteria—structure and dynamics. Springer series in biophysics* (ed. M.-E. Michel-Beyerle), p. 287. Berlin: Springer.

Breton, J., Martin, J. L., Migus, A., Antonetti, A. & Orszag, A. 1986 *Proc. Natn. Acad. Sci. USA* **83**, 5121.

Chan, C.-K., DiMagno, T. J., Chen, L. X.-Q., Norris, J. R. & Fleming, G. R. 1991 *Proc. Natn. Acad. Sci. USA* **88**, 11 202.

Chang, C. H., Tiede, D., Tang, J., Smith, U., Norris, J. & Schiffer, M. 1986 *FEBS Lett.* **205**, 82.

Clayton, R. K. & Sistrom, W. R. (eds) 1978 *The photosynthetic bacteria*. New York: Plenum.

Deisenhofer, J. & Michel, H. 1989 *EMBO J.* **8**, 2149.

Deisenhofer, J., Epp, O., Miki, K., Huber, R. & Michel, H. 1985 *Nature* **318**, 618.

Dressler, K., Umlauf, E., Schmidt, S., Hamm, P., Zinth, W., Buchanan, S. & Michel, H. 1991 *Chem. Phys. Lett.* **183**, 270.

Ermler, U., Fritzsch, G., Buchanan, S. K. & Michel, H. 1994 *Structure* **2**, 925.

Fajer, J., Brune, D. C., Davis, M. S., Forman, A. & Spaulding, L. D. 1975 *Proc. Natn. Acad. Sci. USA* **72**, 4956.

Finkele, U., Dressler, K., Lauterwasser, C. & Zinth, W. 1990 In *Springer series in biophysics: reaction centers of photosynthetic bacteria* (ed. M. E. Michel-Beyerle), vol. 6, p. 127. Berlin: Springer.

Fleming, G. R., Martin, J. L. & Breton, J. 1988 *Nature* **333**, 190.

Frolov, E. N., Goldanski, V. I., Birk, A. & Parak, F. 1996 *Eur. Biophys. J.* **24**, 433.

Holzapfel, W., Finkele, U., Kaiser, W., Oesterhelt, D., Scheer, H., Stilz, H. U. & Zinth, W. 1989 *Chem. Phys. Lett.* **160**, 1.

Holzapfel, W., Finkele, U., Kaiser, W., Oesterhelt, D., Scheer, H., Stilz, H. U. & Zinth, W. 1990 *Proc. Natn. Acad. Sci. USA* **87**, 5168.

Jortner, J. 1976 *J. Chem. Phys.* **64**, 4860.

Kirmaier, C. & Holten, D. 1990 *Proc. Natn. Acad. Sci. USA* **87**, 3552.

Kirmaier, C., Holten, D. & Parson, W. W. 1985 *Biochim. Biophys. Acta* **810**, 33.

Knapp, E. W., Zinth, W., Sander, M., Fischer, S. F. & Kaiser, W. 1985 *Proc. Natn. Acad. Sci. USA* **82**, 8463.

Kuhn, H. 1986 *Phys. Rev.* A **34**, 3409.

Lauterwasser, C., Finkele, U., Scheer, H. & Zinth, W. 1991 *Chem. Phys. Lett.* **183**, 471.

Martin, J. L., Breton, J., Hoff, A. J., Migus, A. & Antonetti, A. 1986 *Proc. Natn. Acad. Sci. USA* **83**, 957.

McDermott, G., Prince, S. M., Freer, A. A., Hawthornthwaite-Lawless, A. M., Papiz, M. Z., Cogdell, R. J. & Isaacs, N. W. 1995 *Nature* **374**, 517.

Michel-Beyerle, M. E., Plato, M., Deisenhofer, J., Michel, H., Bixon, M. & Jortner, J. 1988 *Biochim. Biophys. Acta* **932**, 52.

Schmidt, S., Arlt, T., Hamm, P., Huber, H., Nägele, T., Wachtveitl, J., Meyer, M., Scheer, H. & Zinth, W. 1994 *Chem. Phys. Lett.* **223**, 116.

Schmidt, S., Arlt, T., Hamm, P., Huber, H., Nägele, T., Wachtveitl, J., Zinth, W., Meyer, M. & Scheer, H. 1995 *Spectrochim. Acta,* A **51**, 1565.

Zinth, W., Arlt, T. & Wachtveitl, J. 1996 *Ber. Bunsenges. Phys. Chem.* **100**, 1962.

Zinth, W., Kaiser, W. & Michel, H. 1983 *Biochim. Biophys. Acta* **723**, 128.

Zinth, W., Sander, M., Dobler, J. & Kaiser, W. 1985 In *Antenna and reaction centers of photosynthetic bacteria* (ed. M. E. Michel-Beyerle), p. 97. Berlin: Springer.